Thermal Degradation of Heterogeneous Concrete Materials*

K. Willam, I. Rhee & Y. Xi
University of Colorado at Boulder, USA

ABSTRACT: In this paper we examine the interaction of thermal and mechanical damage processes in heterogeneous materials such as concrete. After a brief introduction of high temperature effects in concrete, we address two topics: (a) the interaction of thermal and mechanical damage at the mesomechanical level of observations, when volumetric and deviatoric degradation take place simultaneously; (b) the effect of thermal expansion and shrinkage in the two-phase concrete material when thermal softening of the elastic properties leads to massive degradation of the load resistance.

1 MOTIVATION

In the aftermath of extreme events in the recent past the performance of cement-based materials has come to forefront in fire safety assessment of tunnels and high rise buildings. An accurate mathematical characterization of cement-based composites, which describes thermal softening and dimensional changes due to changes in the temperature environment has been the focus in the high temperature reactor industry for over thirty years. It is indeed unfortunate that several accidents in the recent past demonstrate the needs for a more comprehensive understanding of cement-based materials exposed to fire environments. A successful predictive model will have great implications for high temperature analysis and design of cement-based material systems with direct implication to fire safety assessment of concrete structures. The main deficiency of current constitutive models is the fact that they are calibrated from isothermal conditions in which the transitional effects of variable temperature, humidity, chemical and mechanical loading are neglected. Moreover, no established theory exists at present how to construct high temperature constitutive relations and cohesive interface properties that are based on micro- and mesostructural features of the adherent bulk materials.

In the back of these fundamental issues on multiscale analysis and design of high temperature materials are the fields of fire protection and fire resistance of cement-based materials. Thereby, the exploratory study is intended as a proof of concept for multi-scale multi-physics engineering to reduce ablation and spall effects in thermal shock problems when fire safety issues are considered.

The performance of cement-based materials under elevated temperatures are very complicated and difficult to characterize. With increasing temperature there is a decrease of compressive strength, density, thermal conductivity, thermal diffusivity in concrete because of increase of porosity and permeability [(Anderberg and Thelandersson 1976),(Thelandersson 1987), (Schneider 1988), (Khoury, Sullivan, and

*accepted for publication in Special Issue on Durability, ASCE Materials Journal, Dec 2002, revised Oct. 2003

Grainger 1985), (Bazant and Chern 1987), (Phan 1996), (Bazant and Kaplan 1996), (Shin, Kim, Kim, Chung, and Jung 2002),(Poon, Azhar, Anson, and Wong 2001). These changes of physical properties are caused by three processes taking place at elevated temperatures:

(a) Phase transformation processes - Loss of free water occurs at about 100 ^{o}C. Decomposition of calcium hydroxide takes place at about 450 ^{o}C. The crystal structure of quartz transforms at 573 ^{o} C from α- to the β- form.

(b) Evolution processes in pore structure - the volume and surface of pores increase up to a temperature of approximately 500 ^{o}C, and decrease with further increase of temperature. The chemical processes result in pore pressures which increase the pore structure and affect the permeability and diffusivity of concrete.

(c) Thermo-hygro-mechanical coupled processes - The thermo-mechanical coupling is associated with the temperature gradient upon rapid heating causing severe thermal stress in concrete leading to dehydration and shrinkage of the cement matrix. The thermo-hygral interaction determines the multiphase transport of water in the liquid, moisture in the vapor, and air in the gaseous phases.

In addition to these three effects, it is the dependence of thermal stress on thermal softening of the elastic properties and the thermal expansion and shrinkage which are responsible for the large reduction of axial stress when confined concrete specimens are subjected to high temperature sweeps $20 \leq T \leq 800^0 C$. Figure 1, which has been reproduced from (Anderberg and Thelanderssson 1976) and (Thelandersson 1987), illustrates the effect of axial restraint on the thermal stress, when the temperature in the concrete specimen increases to very high levels, and when spalling leads to large stress relaxation and sometimes explosive failure. Figure 2 shows the axial expansion indicating that axial expansion reverts to shrinkage at increasing temperature in the presence of axial compression.

Clearly, these transient experiments exhibit a number of inelastic effects such as creep and relaxation, the build-up of vapor pressure and drying shrinkage, as well as phase transformations in the aggregate and the cement paste. However we believe that dependence of the elastic properties and thermal expansion and shrinkage on the temperature is the primary effect which deserves our attention when transient high temperature excursions are considered. For recent studies on high temperature effects on concrete materials we refer the reader to (Ulm, Coussy, and Bažant 1999), (Ulm, Acker, and Lévy 1999), (Nenech, Meftah, and Reynouard 2002), and (Schrefler, Khoury, Gawin, and Majorana 2002).

2 OBJECTIVE AND SCOPE

To start with, let us consider the uniaxial thermo-elastic relationship, when the modulus of elasticity and the thermal coefficient of expansion are functions of temperature,

$$\sigma = E(T)[\epsilon - \alpha(T)\Delta T] \tag{1}$$

where $\Delta T = T(t) - T_o$ denotes the excursion from the reference temperature. Under thermal transients, the 'thermo-hyperelastic' relation translates into the rate form,

$$\dot{\sigma} = E(T)[\dot{\epsilon} - \alpha(T)\Delta\dot{T}] + \dot{E}(T)[\epsilon - \alpha(T)\Delta T] - \dot{\alpha}(T)\, E(T)\Delta T \tag{2}$$

This differs significantly from the 'thermo-hypoelastic' formulation advocated by (Thelandersson 1987), which only retains the first term on the rhs, but not the rate of change of the elastic modulus and that of the thermal expansion. In fact, it is this rate term $\dot{E}(T)$ which is primarily responsible for relaxation of thermal stress when the temperature increases in addition to shrinkage of the cementitious matrix.

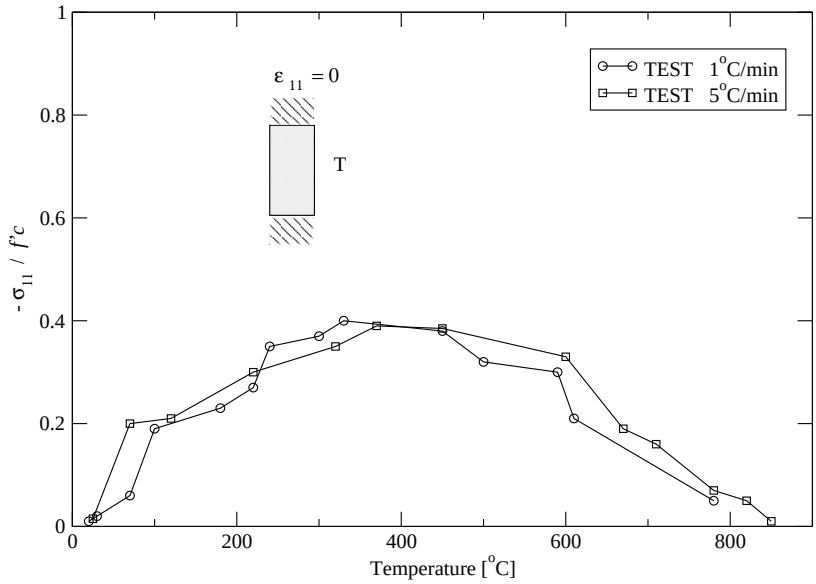

Figure 1: Relaxation of axial stress when restrained concrete specimen is subjected to temperature sweep [Anderberg & Thelandersson, 1976, 1987]

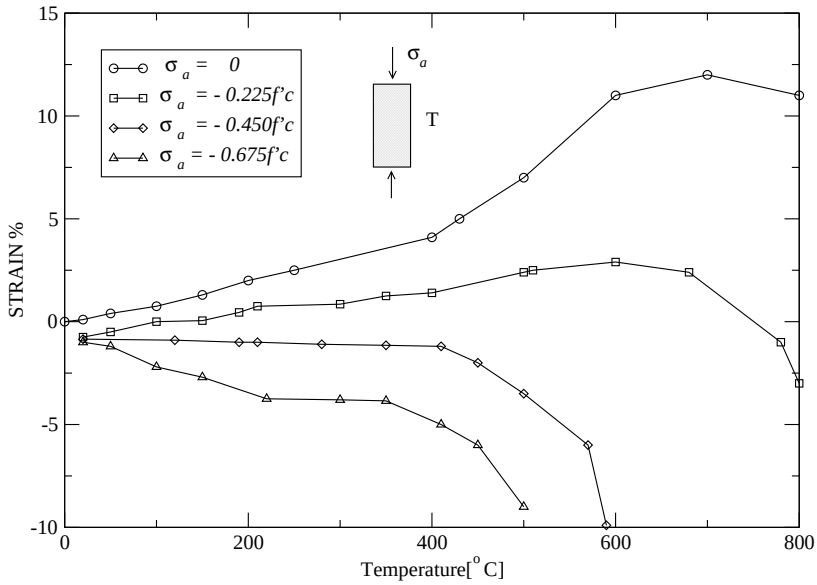

Figure 2: Axial strain when concrete specimen is subjected to temperature sweep at different levels of axial stress σ_a [Anderberg & Thelandersson, 1976, 1987]

2.1 Thermo-elastic Damage

Let us consider the elementary concept of damage which accounts for the variation of the thermo-elastic material properties due to temperature-sensitivity,

$$E(T) = [1 - d_E]\, E^o, \quad \text{and} \quad \alpha(T) = [1 - d_\alpha]\, \alpha^o \tag{3}$$

Here E^o and α^o denote the reference values of the elastic modulus and the coefficient of thermal expansion at room temperature. In this case, the thermo-hyperelastic damage relation writes as,

$$\sigma = [1 - d_E]\, E^o \epsilon - [1 - d_E][1 - d_\alpha]\, E^o \alpha^o \Delta T \tag{4}$$

The rate form thereof involves changes of the external state variables as well as changes of the internal damage variables,

$$\dot{\sigma} = [1 - d_E]\, E^o \dot{\epsilon} - [1 - d_E][1 - d_\alpha]\, E^o \alpha^o \Delta \dot{T} - \dot{d}_E [E^o \epsilon - [1 - d_\alpha] E^o \alpha^o \Delta T] + \dot{d}_\alpha [1 - d_E] E^o \alpha^o \Delta T \tag{5}$$

Considering a temperature sweep under kinematically restrained conditions, the relaxation problem with $\epsilon = 0, \dot{\epsilon} = 0$, results in the governing differential equation for constant thermal expansion when $\dot{d}_\alpha = 0$,

$$\dot{\sigma} - \dot{d}_E [1 - d_\alpha] E^o \alpha^o \Delta T = -[1 - d_E][1 - d_\alpha]\, E^o \alpha^o \Delta \dot{T} \tag{6}$$

The solution of the homogeneous part of the differential equation is an exponential decay function,

$$\sigma(t) = \sigma^o_{th} e^{-\dot{d}_E [t - t_o]} \quad \text{where} \quad \sigma^o_{th} = -[1 - d_\alpha] E^o \alpha^o \Delta T \tag{7}$$

which results in relaxation of the thermal stress when thermal softening prevails, i.e. $\dot{d}_E < 0$. It is this stress relaxation effect which is of primary interest in this study of progressive damage in two-phase materials made of aggregate inclusions embedded in a continuous cement-based matrix.

2.2 Product Format of Thermal and Elastic Damage

In the introductory observation we noted two damage variables, one was associated with the change of thermal expansion, the other with the change of the elastic stiffness with temperature. Under increasing temperature, we may expect an increasing amount of expansion in a homogeneous medium and a reduction of elastic stiffness with increasing temperatures. The question is, whether the two degradation processes are interacting, or whether they are independent of each other. This leads to the issue of additive versus product decomposition of the effective damage variable, which combines the effect of the two damage processes. In other terms, does the effective thermo-mechanical damage variable follow the product format,

$$1 - d = [1 - d_E][1 - d_\alpha] = 1 - d_E - d_\alpha + d_E \cdot d_\alpha \tag{8}$$

or the additive format,

$$1 - d = 1 - d_E - d_\alpha \tag{9}$$

Note the product term $d_E \cdot d_\alpha$ on the rhs of Eq. 8 is the essential difference of the two damage models. In case of very small damage values, when $d_E < 1, d_\alpha < 1$, there is little difference between the two damage formulations since $d_E \cdot d_\alpha << 1$. However, in the case of very large temperature excursions the change of damage may be very significant since the two rate terms of the product law below are no longer of higher order which may be neglected.

$$\dot{d} = \dot{d}_E + \dot{d}_\alpha - \dot{d}_E \cdot d_\alpha - d_E \cdot \dot{d}_\alpha \tag{10}$$

Considering the thermo-elastic stress-strain relation in Eq. 4 it is apparent that the product format is a natural consequence of the temperature dependence in the thermal stress expression. This issue was raised by one of the reviewers on the basis of micromechanical considerations. The review paper by

(Zaoui 2002) led to the seminal papers by (Levin 1967) and by (Rosen and Hashin 1970) dealing with the effective thermal expansion in heterogeneous materials. In summary, the thermal expansion of a two-phase composite is not only the simple volume average of the coefficients of thermal expansion, but also depends on the elastic properties of the two constituents. Using the notation of (Torquato 2000), the effective thermal expansion involves,

$$\alpha_{eff}^{th} =< \alpha > + \frac{\alpha_2 - \alpha_1}{\frac{1}{K_2} - \frac{1}{K_1}} [\frac{1}{K_{eff}} - < \frac{1}{K} >] \tag{11}$$

where $< \alpha >= c_1\alpha_1 + c_2\alpha_2$ denotes the volume average of the simple mixture rule, and where $c_1 + c_2 = 1$ denote the volume fractions of the two phases. Note, the second term on the rhs introduces elastic interactions embodied in the difference of the volume average of the bulk compliance $< \frac{1}{K} >= c_1\frac{1}{K_1} + c_2\frac{1}{K_2}$ and the effective bulk compliance $\frac{1}{K_{eff}}$ of the two-phase composite. Hence, damage of the elastic bulk properties affects the effective thermal expansion and vice versa. This observation supports the product decomposition of damage in Eq. 8.

In analogy to the effective thermal expansion in Eq. 11, the effective shrinkage expression developed by (Xi and Jennings 1997) for cement paste and concrete includes the elastic properties of the constituents. Based on the self-consistent model of (Christensen 1979), the following expression governs the effective shrinkage of the homogenized medium,

$$\epsilon_{eff}^{sh} = \frac{K_1\epsilon_1^{sh}c_1[3K_2 + 4G_2] + K_2\epsilon_2^{sh}c_2[4G_2 + 3K_1]}{K_2[3K_1 + 4G_2] - 4c_1G_2[K_2 - K_1]} \tag{12}$$

Here K_1, K_2 and G_1, G_2 are the bulk and shear moduli of the two-phase composite. Note, the effective shrinkage strain depends on both the shrinkage strains of the two constituents as well as their elastic bulk and shear moduli. Again, the elastic properties of the two phases affect the effective shrinkage properties of the homogenized material in support of the product decomposition of damage in Eq. 8.

2.3 Scope of Paper

In the paper we examine thermal deterioration effects in a heterogeneous two-phase material representative of concrete. After the brief discussion of temperature effects in concrete materials we consider special forms of mechanical and thermal coupling in the product form of volumetric and deviatoric damage. For illustration the degradation formulation is applied to model-based simulations of a two-phase concrete composite made of polygonal aggregate inclusions and a continuous cement matrix. The model problem shows the effect of temperature on the elastic stiffness and the thermal expansion and shrinkage when mismatch of the two-phase material introduces progressive degradation. The numerical simulations illustrate the relaxation of axial stress which is compared with the experimental observations on concrete specimens subjected to a combination of thermal and mechanical load histories, see (Anderberg and Thelanderssson 1976) and (Thelandersson 1987).

3 ISOTROPIC FREE ENERGY EXPANSION

In the subsequent discussion we develop a thermo-mechanical damage model which accounts for thermal softening as well as elastic damage. For conciseness we omit the mass density from the energy potential below and replace the absolute temperature by the relative room temperature. The representation of scalar-valued tensor functions in terms of the irreducible set of three strain invariants,

$(tr\boldsymbol{\epsilon}), (tr\boldsymbol{\epsilon}^2), (tr\boldsymbol{\epsilon}^3)$, and relative temperature $\Delta T = T - T_o$, yields the general form

$$\psi(\boldsymbol{\epsilon}, \Delta T) = \psi^{lin}(\boldsymbol{\epsilon}, \Delta T) + \psi^{nln}(\boldsymbol{\epsilon}, \Delta T) \tag{13}$$

where the monomial terms up to second order describe the linear response.

$$\psi^{lin}(\boldsymbol{\epsilon}, \Delta T) = b_0 + b_1[tr\boldsymbol{\epsilon}] + b_2[\Delta T] + b_3[tr\boldsymbol{\epsilon}]^2 + b_4[tr\boldsymbol{\epsilon}^2] + b_5[\Delta T]^2 + b_6[tr\boldsymbol{\epsilon}][\Delta T] \tag{14}$$

and the higher order terms the nonlinear response,

$$\psi^{nln}(\boldsymbol{\epsilon}, \Delta T) = b_7[tr\boldsymbol{\epsilon}^2][tr\boldsymbol{\epsilon}] + b_8[tr\boldsymbol{\epsilon}^3] + b_9[\Delta T]^3 + b_{10}[tr\boldsymbol{\epsilon}]^2[\Delta T] + b_{11}[tr\boldsymbol{\epsilon}^2][\Delta T] + b_{12}[tr\boldsymbol{\epsilon}][\Delta T]^2 + .. \tag{15}$$

This leads to the stress-strain relationship for isotropic nonlinear thermoelasticity in its general form:

$$\boldsymbol{\sigma} = \frac{\partial \psi}{\partial \boldsymbol{\epsilon}} = \phi_1 \mathbf{1} + \phi_2 \boldsymbol{\epsilon} + \phi_3 \boldsymbol{\epsilon}^2 \tag{16}$$

where **1** denotes the unit second order tensor, and where the response functions depend on the strain invariants and temperature,

$$\phi_1([tr\boldsymbol{\epsilon}], [\Delta T]) = 2b_3[tr\boldsymbol{\epsilon}] + b_6[\Delta T] + b_7[tr\boldsymbol{\epsilon}^2] + 2b_{10}[tr\boldsymbol{\epsilon}][\Delta T] + 2b_{12}[\Delta T]^2 \tag{17}$$

and

$$\phi_2([tr\boldsymbol{\epsilon}], [\Delta T]) = 2b_4 + 2b_7[tr\boldsymbol{\epsilon}] + 2b_{11}[\Delta T] \tag{18}$$

and

$$\phi_3 = 3b_8 \tag{19}$$

We note the appearance of strain and temperature dependent terms in both response functions $\phi_1 = \phi_1([tr\boldsymbol{\epsilon}], [\Delta T])$ and $\phi_2 = \phi_2([tr\boldsymbol{\epsilon}], [\Delta T])$.

For the damage model we restrict our attention to the constitutive format of linear thermo-elasticity where the nonlinear terms $b_7 - b_{12} = 0$, and where the effect of the third invariant is omitted $b_8 = 0$. Thereby it is understood that the nonlinear mechanical and thermal effects are introduced by appropriate damage models for the volumetric and deviatoric components of stress. Using the classical notation for linear isotropic thermo-elasticity, $2b_3 = \Lambda\,, b_6 = -3K\alpha,\, b_4 = G$,

$$\boldsymbol{\sigma} = [\Lambda\,[tr\boldsymbol{\epsilon}] - 3K\alpha\Delta T]\,\mathbf{1} + 2G\,\boldsymbol{\epsilon} \tag{20}$$

Here K denotes the elastic bulk modulus, α the traditional coefficient of thermal expansion, while $\Lambda, G,$ are the Lamé constants of linear elasticity. A convenient way for the thermo-elastic stress-strain relation is to decompose the strain into volumetric and deviatoric components,

$$\boldsymbol{\sigma} = K[\,tr(\boldsymbol{\epsilon} - \boldsymbol{\alpha}\Delta T)]\mathbf{1} + 2\,G\mathbf{e} \quad \text{where} \quad \mathbf{e} = \boldsymbol{\epsilon} - \frac{1}{3}[tr\boldsymbol{\epsilon}]\mathbf{1} \tag{21}$$

where the elastic bulk and shear moduli, K, G and the isotropic coefficient of the second order thermal expansion tensor $\boldsymbol{\alpha} = \alpha\mathbf{1}$ are in general functions of the strain invariants and temperature.

3.1 *Volumetric-Deviatoric Damage*

For constructing a definite thermo-elastic damage model let us start from the Helmholtz free energy per unit volume in terms of elastic strain, temperature and two damage variables for volumetric and deviatoric degradation. Assuming decoupling between the volumetric and deviatoric degradation, the energy contributions of linear elastic behavior (Carol, Rizzi, and Willam 2002) expands into the additive form of volumetric and deviatoric thermo-elastic damage:

$$\psi_{el} = \psi_{vol} + \psi_{dev} = \tfrac{1}{2}[1 - d_{vol}]K^o[tr(\boldsymbol{\epsilon} - \boldsymbol{\alpha}\Delta T)]^2 + [1 - d_{dev}]G^o[tr\mathbf{e}^2] + \tfrac{1}{2}c_v[\tfrac{\Delta T}{T_o}]^2 \tag{22}$$

This expansion leads to the following constitutive statements for

(a) Elastic Stress :

$$\boldsymbol{\sigma} = \frac{\partial \psi}{\partial \boldsymbol{\epsilon}_{el}} = [1 - d_{vol}]K^o[tr(\boldsymbol{\epsilon} - \boldsymbol{\alpha}\Delta T)]\mathbf{1} + [1 - d_{dev}]2\,G^o\mathbf{e} \tag{23}$$

(b) Internal Entropy:

$$s = -\frac{\partial \psi}{\partial \Delta T} = [1 - d_{vol}]K^o[tr\boldsymbol{\alpha}]\Delta T[tr\boldsymbol{\alpha}] + c\frac{\Delta T}{T_o} \tag{24}$$

(c) Conjugate Thermodynamic Forces:

$$\mathcal{Y}_{vol} = -\frac{\partial \psi}{\partial d_{vol}} = \frac{1}{2}K^o[tr(\boldsymbol{\epsilon} - \boldsymbol{\alpha}\Delta T)]^2 \quad \text{and} \quad \mathcal{Y}_{dev} = -\frac{\partial \Psi}{\partial d_{dev}} = G^o[tr\mathbf{e^2}] \tag{25}$$

(d) Reduced Dissipation Inequality :

$$\dot{\mathcal{D}} = \boldsymbol{\sigma} : \dot{\boldsymbol{\epsilon}} - \dot{\psi} = \mathcal{Y}_{vol}\,\dot{d}_{vol} + \mathcal{Y}_{dev}\,\dot{d}_{dev} \geq 0 \tag{26}$$

which is satisfied when $\dot{d}_{vol} > 0$, and $\dot{d}_{dev} > 0$ since the thermodynamic forces are strictly positive because of their quadratic forms.

Volumetric damage is primarily due to thermal dependence of the bulk modulus and the coefficient of thermal expansion, $K = K(\Delta T), \alpha = \alpha(\Delta T)$. We describe thermo-elastic damage by the product representation discussed in Section 2.2, where

$$[1 - d_{vol}] = [1 - d_K][1 - d_\alpha] \quad \text{where} \quad d_K = 1 - \frac{K(\Delta T)}{K^o} \quad \text{and} \quad d_\alpha = 1 - \frac{\alpha(\Delta T)}{\alpha^o} \tag{27}$$

In contrast to the volumetric expansion we assume that the deviatoric degradation of the shear modulus is primarily due to mechanical damage and thermal softening,

$$G(\Delta T, \mathbf{e}) = [1 - d_{dev}]G^o, \quad \text{where} \quad d_{dev} = [1 - \frac{G(\mathbf{e})}{G^o}][1 - \frac{G(\Delta T)}{G^o}] \tag{28}$$

For the sake of simplicity we assume decoupling of volumetric and deviatoric damage. In this case, two independent damage functions define the onset of volumetric and deviatoric degradation,

$$F_{vol} = f(\mathcal{Y}_{vol}) - r(d_{vol}) \leq 0 \quad \text{and} \quad F_{dev} = f(\mathcal{Y}_{dev}) - r(d_{dev}) \leq 0 \tag{29}$$

In the simplest case the energy demand is expressed in terms of the thermodynamic force, $f(\mathcal{Y}_{vol}) = \mathcal{Y}_{vol}, f(\mathcal{Y}_{dev}) = \mathcal{Y}_{dev}$, and the resistance by the two energy capacity functions:

$$r_{vol} = \frac{1}{2}[1 - d_{vol}]K^o[tr(\boldsymbol{\epsilon} - \boldsymbol{\alpha}\Delta T)]^2 \quad \text{and} \quad r_{dev} = r^o_{dev}[1 - d_{dev}]^{p_{dev}-1} \tag{30}$$

The mechanical part of the deviatoric damage resistance is expressed in terms of the fracture energy release rate per unit volume, g_f^{II}, and the characteristic deviatoric length l_{dev},

$$r^o_{dev} = \frac{1}{2}\tau^o_s\gamma^o_s = \frac{1}{2}\frac{[\tau^o_s]^2}{G^o} \quad \text{and} \quad p_{dev} = \frac{r^o_{dev}}{g_f^{II}/l_{dev}} < 1 \tag{31}$$

Under persistent damage, the two independent loading conditions, lead to the two consistency conditions $\dot{F}_{vol} = 0, \dot{F}_{dev} = 0$, which are assumed to remain decoupled for the sake of simplicity:

$$\dot{F}_{vol} = \dot{\mathcal{Y}}_{vol} - \frac{\partial r_{vol}}{\partial d_{vol}}\dot{d}_{vol} = 0 \quad \text{and} \quad \dot{F}_{dev} = \dot{\mathcal{Y}}_{dev} - \frac{\partial r_{dev}}{\partial d_{dev}}\dot{d}_{dev} = 0 \tag{32}$$

These two key equations provide the rate equations of volumetric and deviatoric degradation in terms of the rate of the thermodynamic forces, where

$$\dot{\mathcal{Y}}_{vol} = K^o[tr(\boldsymbol{\epsilon} - \boldsymbol{\alpha}\Delta T)][tr(\dot{\boldsymbol{\epsilon}} - \boldsymbol{\alpha}\Delta\dot{T})] \tag{33}$$

Assuming linear dependence of the bulk modulus and the thermal expansion on the temperature,

$$K(T) = K^o[1 - h_K\Delta T] \quad \text{and} \quad \alpha(T) = \alpha^o[1 - h_\alpha\Delta T] \tag{34}$$

the evolution of volumetric damage due to temperature transients,

$$\dot{d}_{vol} = h_{vol}\Delta\dot{T} = \dot{d}_K[1 - d_\alpha] + \dot{d}_\alpha[1 - d_K] \tag{35}$$

involves,

$$\begin{gathered}\dot{d}_K = -\frac{1}{K_o}\frac{\partial K}{\partial T}\Delta\dot{T} = h_K\Delta\dot{T} \\ \dot{d}_\alpha = -\frac{1}{\alpha_o}\frac{\partial \alpha}{\partial T}\Delta\dot{T} = h_\alpha\Delta\dot{T} \\ h_{vol} = h_K[1 - h_\alpha\Delta T] + h_\alpha[1 - h_K\Delta T]\end{gathered}$$

In contrast, the rate of the deviatoric thermodynamic force,

$$\dot{\mathcal{Y}}_{dev} = 2G^o\mathbf{e} : \dot{\mathbf{e}} \tag{36}$$

may mobilize both mechanical as well as thermal softening effects, such that

$$\dot{d}_{dev} = \frac{2G^o}{\mathcal{H}_{dev}}\mathbf{e} : \dot{\mathbf{e}} \quad \text{where} \quad \mathcal{H}_{dev} = \frac{\partial r_{dev}}{\partial d_{dev}} \tag{37}$$

3.2 *Rate Form of Thermo-elastic Damage*

Differentiating the total stress-strain-damage relation in Eq. 23 we obtain the rate of stress,

$$\dot{\boldsymbol{\sigma}} = [1 - d_{vol}]K^o[tr(\dot{\boldsymbol{\epsilon}} - \boldsymbol{\alpha}\Delta\dot{T})]\mathbf{1} - \dot{d}_{vol}K^o[tr(\boldsymbol{\epsilon} - \boldsymbol{\alpha}\Delta T)]\mathbf{1} + [1 - d_{dev}]2\,G^o\dot{\mathbf{e}} - \dot{d}_{dev}2\,G^o\mathbf{e} \tag{38}$$

Substituting the rate of thermo-elastic damage yields the stress rate in terms of strain and temperature rates,

$$\dot{\boldsymbol{\sigma}} = [1 - d_{vol}]K^o[\mathbf{1}\otimes\mathbf{1}] : [\dot{\boldsymbol{\epsilon}} - \boldsymbol{\alpha}\Delta\dot{T}] + \left[[1 - d_{dev}]2\,G^o\mathbb{1} - \frac{4\,G_o^2}{\mathcal{H}_{dev}}\mathbf{e}\otimes\mathbf{e}\right] : \dot{\mathbf{e}} - h_{vol}K^o[tr(\boldsymbol{\epsilon} - \boldsymbol{\alpha}\Delta T)]\mathbf{1}\Delta\dot{T} \tag{39}$$

This may be cast into the tangential stiffness relation below:

$$\boxed{\dot{\boldsymbol{\sigma}} = \mathbb{K}_{ed}^{tan} : [\dot{\boldsymbol{\epsilon}} - \boldsymbol{\alpha}\Delta\dot{T}] + \mathbb{G}_{ed}^{tan} : \dot{\mathbf{e}} - \beta_{vol}\mathbf{1}\Delta\dot{T}} \tag{40}$$

where the tangential bulk modulus tensor is defined as,

$$\mathbb{K}_{ed}^{tan} = [1 - d_{vol}]K^o\mathbf{1}\otimes\mathbf{1} \tag{41}$$

The volumetric stress involves the temperature dependent material properties,

$$\beta_{vol} = h_{vol}K^o[tr(\boldsymbol{\epsilon} - \boldsymbol{\alpha}\Delta T)] \tag{42}$$

Consequently, the volumetric stress-strain rate relation involves a strain driven and a temperature driven component,

$$\dot{\boldsymbol{\sigma}}_{vol} = [\dot{\sigma}_{vol}^{\epsilon} - \dot{\sigma}_{vol}^{T}]\mathbf{1} \tag{43}$$

where

$$\dot{\sigma}_{vol}^{\epsilon} = K^o[1 - d_{vol}][tr\dot{\boldsymbol{\epsilon}}] \tag{44}$$

and

$$\dot{\sigma}_{vol}^{T} = [[1 - d_{vol}] - h_{vol}\Delta T]\,[tr\boldsymbol{\alpha}][\Delta\dot{T}] \tag{45}$$

The second term on the rhs reflects the temperature dependence of the bulk modulus and the coefficient of thermal expansion inherent in h_{vol}.

The deviatoric stress-strain rate relationship has the canonical form,

$$\boxed{\dot{\mathbf{s}} = \mathbb{G}_{ed}^{tan} : \dot{\mathbf{e}}} \tag{46}$$

where the tangential shear stiffness tensor,

$$\mathbb{G}_{ed}^{tan} = [1 - d_{dev}]2\,G^o\mathbb{1} - 2\,G^o h_{dev}\mathbf{e}\otimes\mathbf{e} \tag{47}$$

involves the unit fourth order tensor $\mathbb{1}$ and exhibits strain-induced anisotropy in the form of the symmetric dyadic product, $\mathbf{e}\otimes\mathbf{e}$. Thereby the rate of change of deviatoric energy with regard to shear damage is characterized by the hardening variable,

$$h_{dev} = \frac{2G^o}{\mathcal{H}_{dev}} \quad \text{and} \quad \mathcal{H}_{dev} = \frac{\partial r_{dev}}{\partial d_{dev}} = -r_{dev}^o[p_{dev} - 1][1 - d_{dev}]^{p_{dev}-2} \tag{48}$$

4 MODEL PROBLEM

For illustration we consider the two-phase composite in Figure 3 which depicts polygonal aggregate inclusions embedded in a continuous cement matrix within a 2-D representative volume element, (Willam, Stankowski, Runesson, and Sture 1990). The unit RVE made up 1233 simplex elements interconnected by 1137 nodes is subjected to a transient temperature sweep assuming plane strain (the actual size $14 \times 14\,mm$ of the RVE is of no consequence in this simulation). Kinematic boundary conditions restrain the movement of the nodes at the top and bottom surfaces where adiabatic conditions are imposed preventing heat flow. The specimen is free to expand laterally where a convective boundary layer permits heat ingress during the temperature sweep when the ambient temperature was increased from 20^oC to 770^oC at a rate of $3^oC/min$. The thermomechanical response analysis is carried out with the implicit Galerkin algorithm ($\alpha = \frac{2}{3}$) considering one-way coupling between the transient heat transfer results and the mechanical damage response using 250 time steps of $\Delta t = 60\,sec$. The volumetric and deviatoric properties of the cement matrix depend not only on temperature but also on the level of deviatoric deformations, while the aggregate inclusions are assumed to behave linearly with stress.

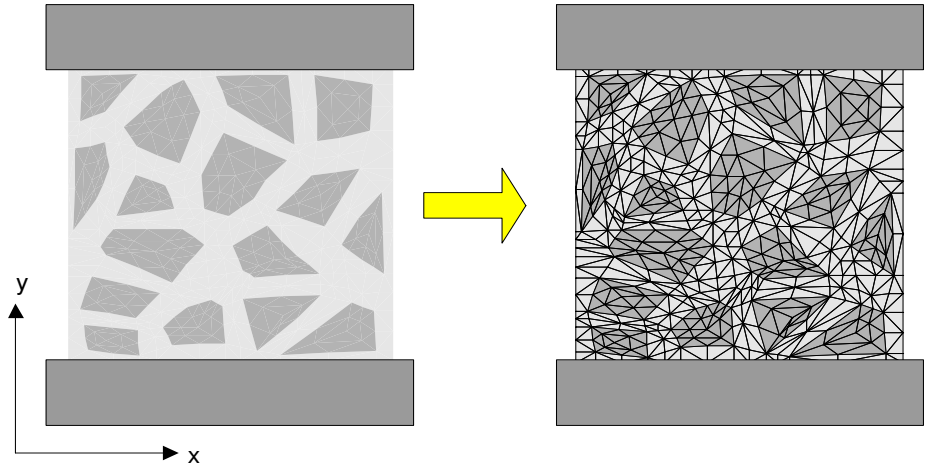

Figure 3: Two-phase particle RVE subjected to vertical confinement during external temperature sweep

The objective of the exercise is to explore the heterogeneous effects of mechanical and thermal degradation in the two-phase composite when thermal and mechanical mismatch leads to different levels of damage in the aggregate particles and the cement matrix. The overall effects are evaluated primarily in the form of relaxation of the thermal stress due to the axial restraints at the top and bottom surfaces which may be compared with the experimental trends reported by Anderberg & Thelandersson [1976, 1987] see Figure 1. This exploratory study investigates the importance of coupling of thermoelastic damage and the relative magnitude of volumetric versus deviatoric damage in addition to their interaction.

4.1 *Mechanical Properties of Aggregate and Cement Matrix*

The temperature dependence of the elastic properties of aggregate and cement matrix are taken from (Khoury, Sullivan, and Grainger 1985) and (Bazant and Kaplan 1996) together with that for the coefficient of thermal expansion.

- Temperature Dependence of Elastic Modulus : E=E_0[0.03921+$e^{-0.002T}$]
  where reference values are for the cement matrix $E_m = E_0$=25000 MPa, and for the aggregate

inclusions $E_a = E_0$=75000 MPa.

Figure 4 illustrates the degradation of the elastic stiffness properties with increasing temperature. Figure 5 shows the corresponding variation of elastic damage which exhibits monotonically in-

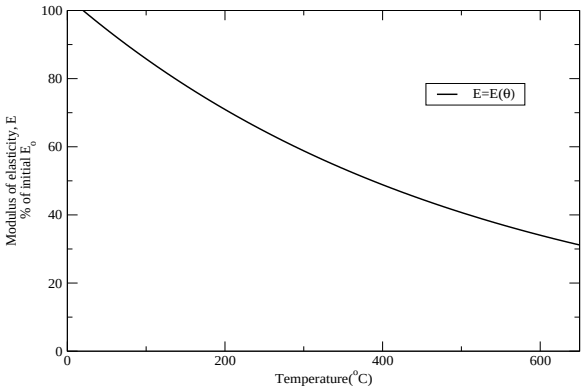

Figure 4: Reduction of elastic modulus with rising temperature, $E = E(T)$

creasing values with increasing temperature up to $d_E \to 0.5$ at $\Delta T = 800^o C$.

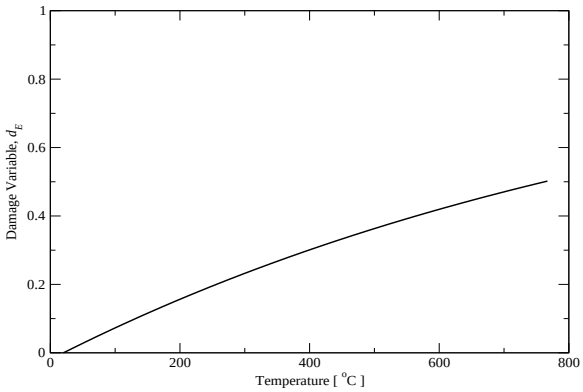

Figure 5: Change of elastic damage variable with temperature, $d_E = 1 - \frac{E(T)}{E^o}$

Assuming that Poisson's ratio exhibits little temperature sensitivity, ν_m=ν_a=0.2, the temperature variation of the elastic modulus defines that of the bulk and shear moduli.

$$G(T) = \frac{E(T)}{2[1+\nu]} \quad \text{and} \quad K(T) = \frac{E(T)}{3[1-2\nu]} \tag{49}$$

The mechanical nonlinearity of the deviatoric response initiates when the octahedral shear stress reaches the critical value τ_o=7.0 MPa in the energy resistance r_o expression Eq. 31. From this point on the fracture energy release rate g_f^{II}=2.20 N/mm, and the characteristic length l_{dev}=1.0 mm describe the nonlinear shear behavior detailed in Eqs. 31 and 48. The corresponding increase of deviatoric damage is shown in Figure 6 which illustrates rapid degradation of the deviatoric stiffness between $100 < T < 300^o C$.

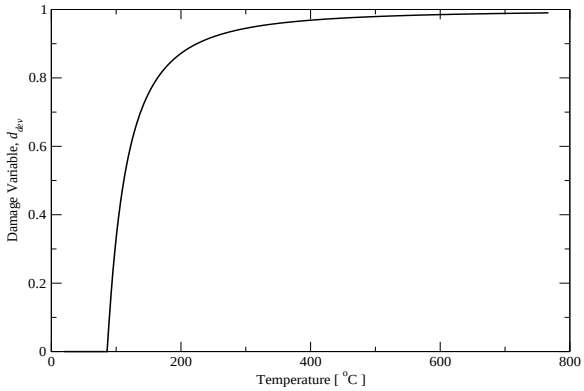

Figure 6: Change of deviatoric damage with temperature and strain, $d_{dev} = [1 - d_G][1 - d_\alpha]$

- Coefficient of Thermal Expansion:

  Normally the coefficients of thermal expansion increase with raising temperature. Assuming no phase transformations and shrinkage due to latent heat effects, the expansion of aggregate inclusions is described by,
  (i) Aggregate Inclusions: α_a=α_a^o($e^{0.05T/100}$-0.01), where α_a^0=9.0 $\times$ 10^{-6}/C.

  In the case of the cement matrix we adopt the format proposed by (**?**), which incorporates shrinkage effects in the effective coefficient of thermal expansion. In this case,
  (ii) Cement Matrix: α_m= 0.00555557α_m^0(200-T), where α_m^0=15.5 $\times$ 10^{-6} /C.

  Figure 7 illustrates the effect of increasing aggregate expansion with raising temperature.

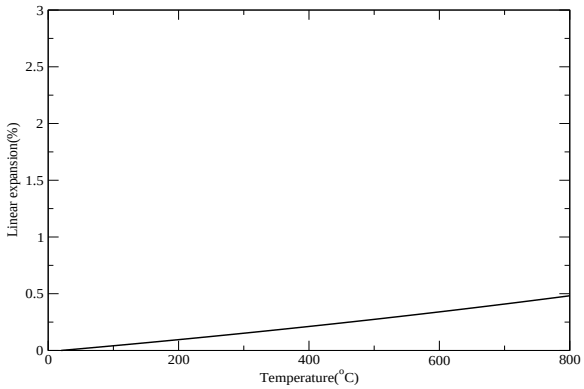

Figure 7: Change of thermal expansion of aggregate inclusions [%] with increasing temperature.

Figure 8. shows the thermal expansion of the cement matrix modified to include the effect of shrinkage. The opposing effects of expansion and shrinkage result in an overall decrease of the coefficient of expansion with increasing temperature. Figure 9 illustrates the corresponding variation of the damage variable d_α for the expanding aggregate inclusions and for the shrinking cement matrix.

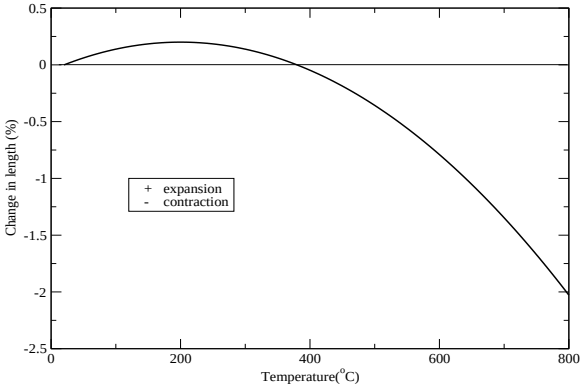

Figure 8: Change of length of cement matrix including shrinkage [%] with increasing temperature.

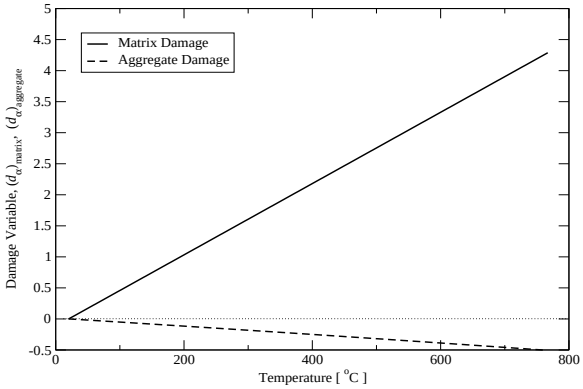

Figure 9: Thermal damage variables $d_\alpha = 1 - \frac{\alpha(T)}{\alpha^o}$
for expanding aggregate and shrinking matrix with increasing temperature.

4.2 *Heat Transfer of Aggregate and Cement Matrix*

In the case of one-way coupling the heat transfer analysis of the RVE may be treated separately from the mechanical degradation analysis. The Gough-Joule effect of mechanical cooling and the mechanical damage of the heat capacity has little influence on the transient heat transfer results which are dominated by convective boundary conditions at the lateral surfaces.

- Aggregate Inclusions:
  Thermal conductivity, k_a = 2.4 $\times$ 10^{-3} kW/(mm·C), Convection coefficient, h_a = 0.0 kW/(mm^2 ·C), Specific heat, c_a = 1170 (kW · h)/(kg ·C), Mass density, ρ_a = 1.92 $\times$ 10^{-6} kg/mm^3.

- Cement Matrix:
  Thermal conductivity, k_m = 10^{-4} kW/(mm·C), Convection coefficient, h_m = 2$\times 10^{-5}$ kW/(mm^2 ·C), Specific heat, c_m = 1170 (kW · h)/(kg ·C), Mass density, ρ_m = 1.92 $\times$ 10^{-6} kg/mm^3.

4.3 *Thermal Degradation of Two-Phase RVE under Thermal Sweep*

The main results of the thermal sweep analysis of the RVE are shown in Figures 10, 11, 12 and 13 which depict the temperature and the axial stress distributions when the ambient temperature reaches

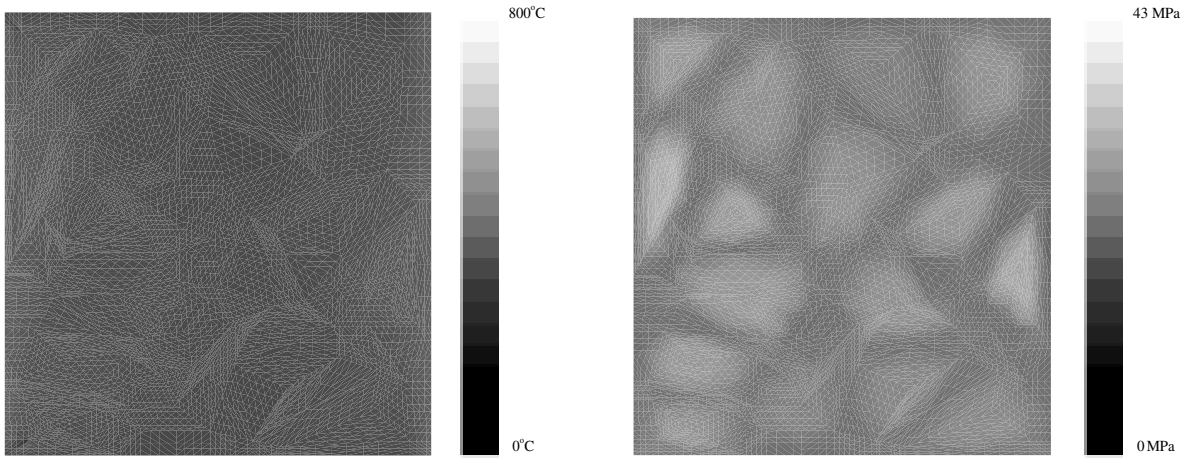

Figure 10: Distribution of temperature and axial stress in RVE at ambient temperature=200^o C

$\Delta T = 200, 400, 600, 800^o$ C. The figures illustrate the heterogeneous effects of the aggregate inclusions and the build up of axial thermal stress on a scale which has been normalized with regard to the maximum values. We note that the high temperature gradient leads to excessive axial stresses at the mid height of the free side surfaces which are responsible for spalling.

Figures 14, 15 and 16 illustrate the axial stress σ_{yy} near the top corner of the restrained RVE specimen. The figures compare the predictions of separate volumetric and deviatoric degradation as well as their combined effect on axial stress. Qualitatively, the trends of the combined volumetric and the deviatoric damage effects are similar and reproduce the overall stress reversal shown in Figure 1 at high temperatures. It is intriguing that the strong thermal degradation of volumetric damage due to shrinkage leads to values of $d_\alpha > 2$, however the combined effect remains within the usual range of $0 \leq d_{vol} \leq 1$. On the other hand the elastic degradation due to deviatoric damage leads to a nonlinear effect when the ambient temperature reaches 100^o C. In both cases of volumetric and deviatoric damage we note that the maximum thermal stress occurs in the range of $300 - 500^o$ C. Degradation of the volumetric stiffness and thermal aggregate expansion as well as shear degradation due to temperature dependence and mechanical damage reduce the maximum level of axial stress. Similarly, the combined effect of volumetric and deviatoric degradation reduces the maximum level of axial stress significantly below the values due to separate volumetric and deviatoric damage.

On a final note, Figure 17 depicts the effect of no shrinkage upon stress relaxation by replacing the shrinkage properties of the cement matrix by the thermal expansion of the aggregate inclusions. Comparing the thermal stress response with that in Figure 16 illustrates the pronounced effect of matrix expansion versus matrix shrinkage, (Khoury, Sullivan, and Grainger 1985). The large increase of thermal damage in Figure 9 is mainly responsible for the large difference of the response behavior in Figures 16 and 17. We should keep in mind that the reduction of the elastic damage by $\sim 50\%$ is fairly small, see Figures 4 and 5 compared the amount of damage due to matrix shrinkage. The relaxation of the axial stress level would have been much higher if the elastic stiffness would have diminished to zero, $E(T = 800) \rightarrow 0$ when $d_E \rightarrow 1$.

5 CONCLUSIONS

The paper addressed subtle issues when the linear coefficient of thermal expansion was augmented by thermal damage variables to account for temperature sensitivity. In addition we focused on the ques-

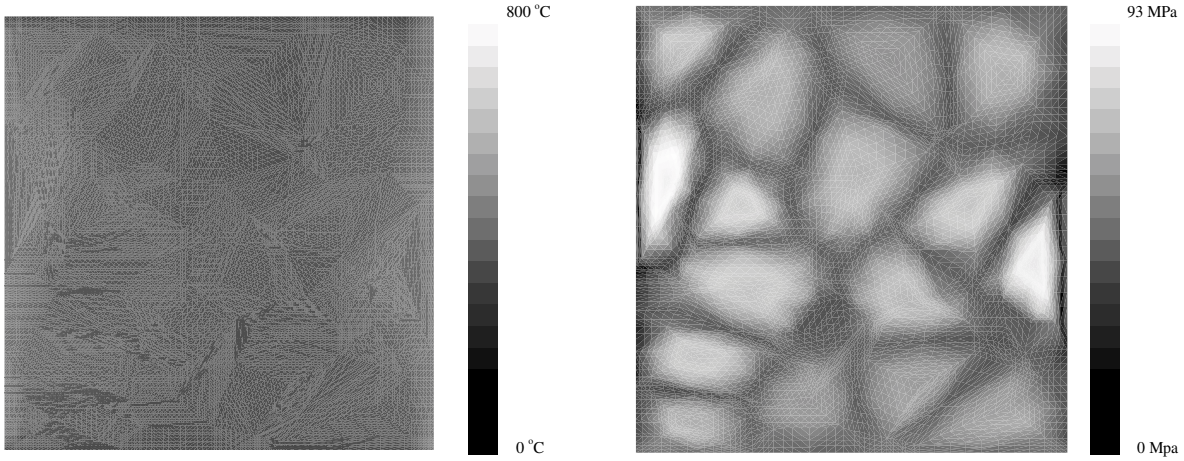

Figure 11: Distribution of temperature and axial stress in RVE at ambient temperature=400^o C

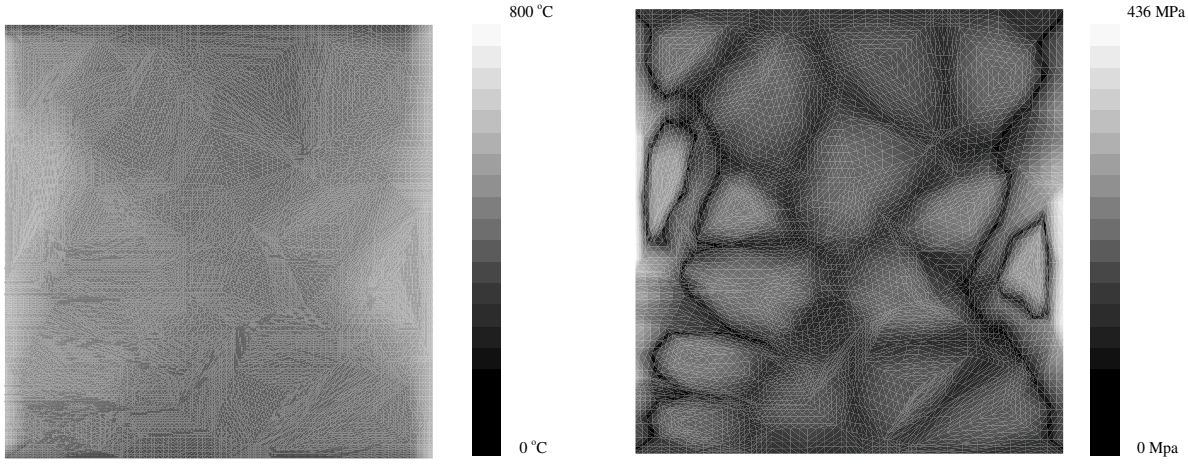

Figure 12: Distribution of temperature and axial stress in RVE at ambient temperature=600^o C

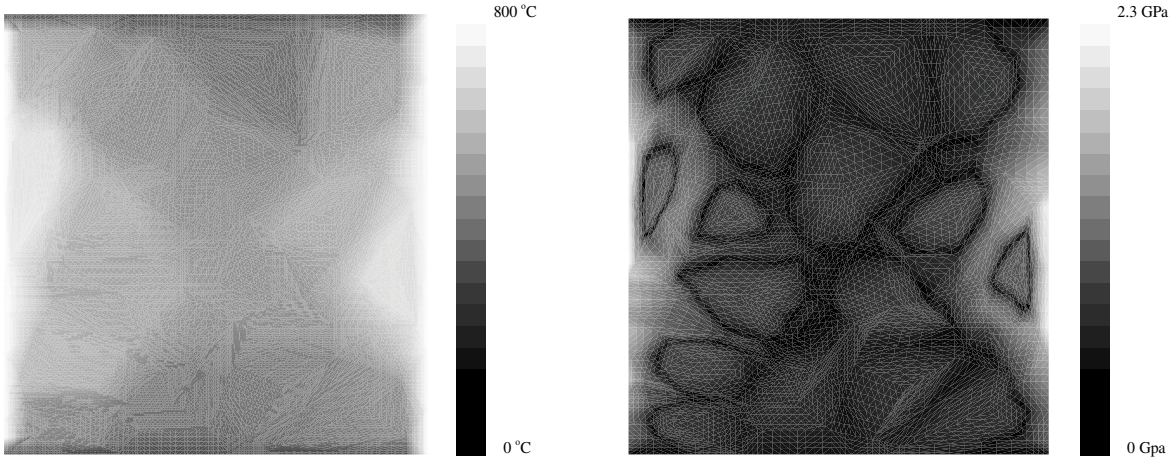

Figure 13: Distribution of temperature and axial stress in RVE at ambient temperature=800^o C

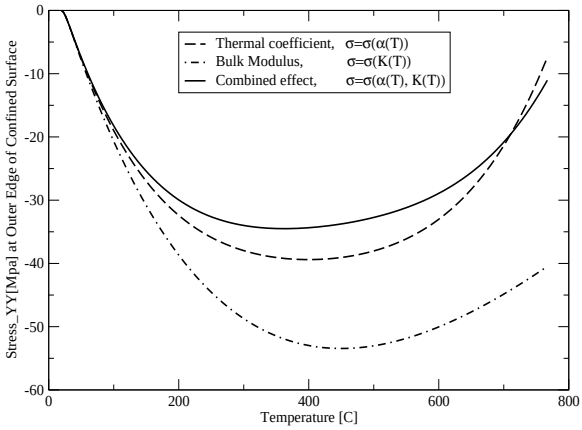

Figure 14: Axial stress relaxation due to volumetric damage

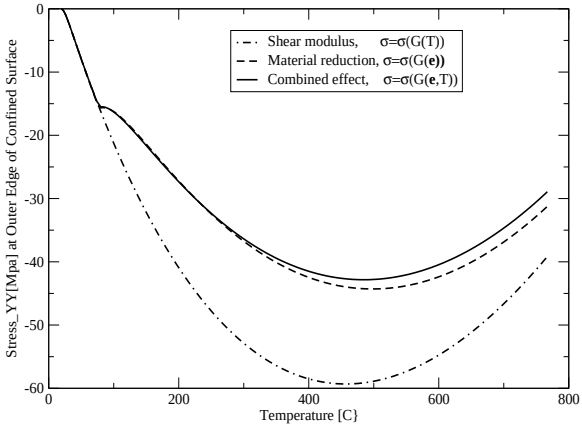

Figure 15: Axial stress relaxation due to deviatoric damage

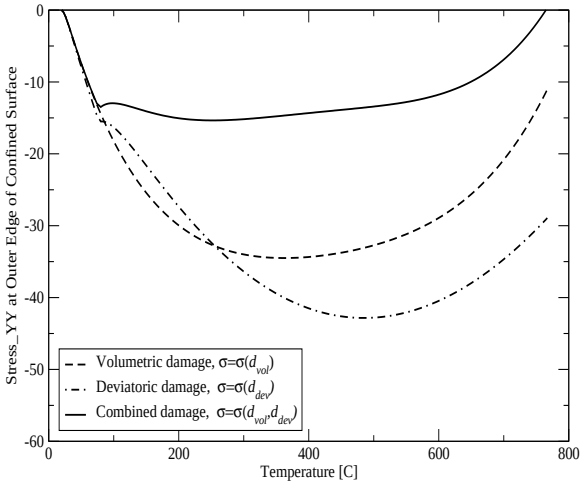

Figure 16: Axial stress relaxation due to combined volumetric-deviatoric damage

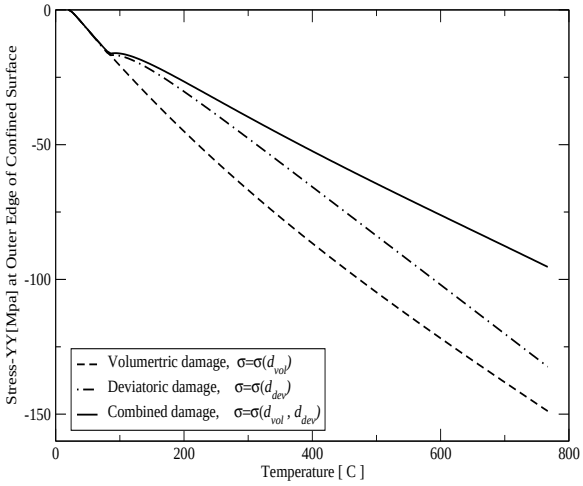

Figure 17: Axial stress relaxation without matrix shrinkage

tion of thermo-mechanical coupling when volumetric-deviatoric damage incorporates thermal as well as mechanical degradation in a rational manner. These two effects result in severe relaxation of thermal stresses due to axial restraints under the thermal sweep. Thereby, it is the combination of both thermal and mechanical degradation processes which drives the relaxation of axial thermal stress, whereby the increasing thermal expansion is counteracted by matrix shrinkage and thermal softening of the elastic properties. The exploratory meso-mechanical study demonstrates the effect of heterogeneity and the important need for more sophisticated hygro-thermal investigations including phase transformations in which the formation of vapor pressure and thermal barriers are considered to understand the fundamental processes behind spalling.

6 ACKNOWLEDGEMENTS

The authors thank the reviewers for their insightful and thought-provoking discussion. One reviewer argued that micromechanical considerations lead to a product decomposition only when damage evolves at two different length scales of observation. Hence the additive decomposition of damage is more appropriate since the thermal and mechanical damage processes evolve at the same mesoscale of observation. The other reviewer queried the origin of the thermal shrinkage effect proposed by (Khoury, Sullivan, and Grainger 1985) for the cement matrix illustrated in Figure 8. His/her question was certainly very appropriate since the corresponding large increase of thermal damage in Figure 9 is mainly responsible for the large difference of the response behavior with and without shrinkage shown in Figures 16 and 17.

The authors wish to acknowledge partial support of this research by the US National Science Foundation under grants CMS 9872379 and CMS-0084598. Opinions expressed in this paper are those of the authors and do not necessarily reflect those of the sponsor.

REFERENCES

Anderberg, Y. and J. Thelanderssson (1976). Stress and deformation characteristics of concrete at high temperatures. Technical report, Lund Institute of Technology, Lund, Sweden.

Bazant, Z. and J.-C. Chern (1987). Stress-induced thermal shrinkage strain in concrete. *Journal of Engineering Mechanics, ASCE 113*(10), 1493–1511.

Bazant, Z. and M. Kaplan (1996). *Concrete at High Temperatures, Material Properties and Mathematical Models*. Burnt Mill, England: Longman Group Limited.

Carol, I., E. Rizzi, and K. Willam (2002). An 'extended' volumetric/deviatoric formulation of anisotropic damage based on a pseudo-log rate. *European Journal of Mechanics -A/Solids 21*, 747–772.

Christensen, R. (1979). *Mechanics of Composite Materials*. New York: Wiley Interscience, Boca Baton.

Khoury, G., P. Sullivan, and B. Grainger (1985). Transient thermal strain of concrete: Literature review, conditions within specimen and individual constituent behaviour. *Magazine of Concrete Research 37*(132), 131–144.

Levin, V. (1967). Thermal expansion coefficients of heterogeneous materials (in russian). *Mekh. Tverd. Tela 8*, 38–94.

Nenech, W., F. Meftah, and J. Reynouard (2002). An elasto-plastic damage model for plain concrete subjected to high temperatures. *Engineering Structures 24*, 597–611.

Phan, L. (1996). Fire performance of high strength concrete: A report of the state-of-the-art. Technical report, Building and Fire Research Laboratory, National Institute of Standards and Technology, Maryland.

Poon, C.-S., M. Azhar, M. Anson, and Y.-L. Wong (2001). Comparison of the strength and durability performance of normal and high strength pozzolanic concretes at elevated temperatures. *Cement and Concrete Resaerch 31*, 1291–1300.

Rosen, B. and Z. Hashin (1970). Effective thermal expansion coefficients and specific heats of composite materials. *International Journal for Engineering Science 8*, 157–173.

Schneider, U. (1988). Concrete at high temperature - a general review. *Fire Safety Journal 13*(1), 55–68.

Schrefler, B., G. Khoury, D. Gawin, and C. Majorana (2002). Thermo-hydro-mechanical modelling of high performance concrete at high temperatures. *Engineering Computations 19*(7), 787–819.

Shin, K.-Y., S.-B. Kim, J.-H. Kim, M. Chung, and P.-S. Jung (2002). Thermo-physical properties and transient heat transfer of concrete at elevated temperature. *Nuclear Engineering and Design 212*, 233–241.

Thelandersson, S. (1987). Modeling of combined thermal and mechanical action in concrete. *Journal of Engineering Mechanics, ASCE 113*(6), 893–906.

Torquato, S. (2000). *Random Heterogeneous Materials, Microstructure and Macrodcopic Properties*. New York: Springer-Verlag.

Ulm, F.-J., P. Acker, and M. Lévy (1999). The *"chunnel"* fire ii: analysis of concrete damage. *Journal of Engineering Mechanics, ASCE 125*(3), 283–289.

Ulm, F.-J., O. Coussy, and Z. Bažant (1999). The *"chunnel"* fire i: chemoplastic softening of rapidly heated concrete. *Journal of Engineering Mechanics, ASCE 125*(3), 272–282.

Willam, K., T. Stankowski, K. Runesson, and S. Sture (1990). *Simulation Issues of Distributed and Localized Failure Computations, Proceedings on Cracking and Damage-Strain Localization and Size Effects*. London and New York: Mazars, J. and Bažant, Z. Eds., Elsevier Applied Sciences.

Xi, Y. and H. Jennings (1997). Shrinkage of cement paste and concrete modelled by a multiscale effective homogeneous theory. *Materials and Structures 30*, 329–339.

Zaoui, A. (2002). Continuum micromechanics: Survey. *Journal of Engineering Materials, ASCE 128*(8), 808–816.